

REPORT No. 564

TESTS OF A WING-NACELLE-PROPELLER COMBINATION AT SEVERAL PITCH SETTINGS UP TO 42°

By RAY WINDLER

SUMMARY

A 4-foot model of Navy propeller No. 4412 was tested in conjunction with an N. A. C. A. cowled nacelle mounted ahead of a thick wing in the 20-foot propeller-research tunnel. A range of propeller pitches from 17° to 42° at $0.75R$ was covered, and for this propeller the efficiency reached a maximum at a pitch setting of 27° ; at higher pitches the efficiencies were slightly lower. The corrected propulsive efficiency is shown to be independent of the angle of attack for the high-speed and the climbing ranges of flight. A working chart is presented for the selection of similar propellers over a wide range of airplane speed, engine power, and propeller revolution speed.

INTRODUCTION

Of the numerous N. A. C. A. reports on the characteristics of metal propellers, probably the most widely used is reference 1, which provides working charts for the selection of propellers for use with engines located in the various shapes of fuselages commonly used at the time of publication. A sufficient range of airplane speed, engine power, propeller pitch, and propeller revolution speed was covered in these tests to meet and even to exceed the needs at that time. The recent increase in high speed and the use of more highly powered and of geared engines has, however, necessitated additional propeller tests.

Current research of the N. A. C. A. on wing-nacelle-propeller arrangements, confined mainly to a propeller pitch of 17° at $0.75R$, has shown that position B of reference 2, with the nacelle located in line with and about 30 percent of the chord ahead of the leading edge of the wing, is one of the desirable combinations for use with radial engines. Accordingly, this position was selected for an extension of the program to include tests of a propeller-pitch range from 17° to 42° at $0.75R$. The subject paper presents the results of these tests in a form suitable for the selection of a propeller for a wide range of conditions; the results cover the present needs as well as some future possibilities.

APPARATUS AND METHODS

The tests were conducted in the N. A. C. A. 20-foot propeller-research tunnel (reference 3). The wing of

5-foot chord and 15-foot span, the nacelle, and the propeller described in reference 2 were used. The single sting was replaced by a double one with offsets at the rear, partly for convenience and partly to secure a larger negative angle of attack. (See fig. 1.)

The method of testing was similar to that of reference 2 except that tare runs were omitted because previous tests had shown that the tare was independent of lift and therefore not required in the analysis. The wing was tested for airfoil characteristics from -10° to 10° angle of attack with and without the nacelle. Propeller tests were then made with propeller pitches

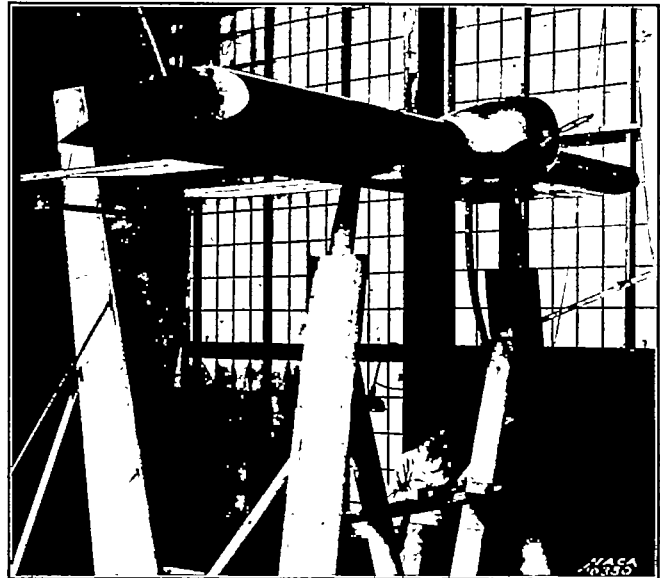


FIGURE 1.—Test set-up.

from 17° to 42° at $0.75R$ for wing angles of attack from -8° to 5° .

The V/nD range for each pitch was obtained in the following manner: A revolution speed was set that would require about the maximum torque of the motor at the ground point. This revolution speed was held constant and the air speed gradually increased up to about 102 miles per hour. In order to obtain the higher values of V/nD , the air speed was held at 102 miles per hour and the revolution speed decreased. The following values of propeller speed (within ± 15

r. p. m.) were used for the constant revolution-speed portion of the tests.

Pitch at 0.75R.	Propeller speed
Degrees	r. p. m.
17	2,800
22	2,300
27	1,950
32	1,700
37	1,475
42	1,400

RESULTS

These results are presented in the same graphic and tabular form as in previous wing-nacelle reports. A detailed discussion of the accuracy and manner of presentation may be found in references 2 and 4. The

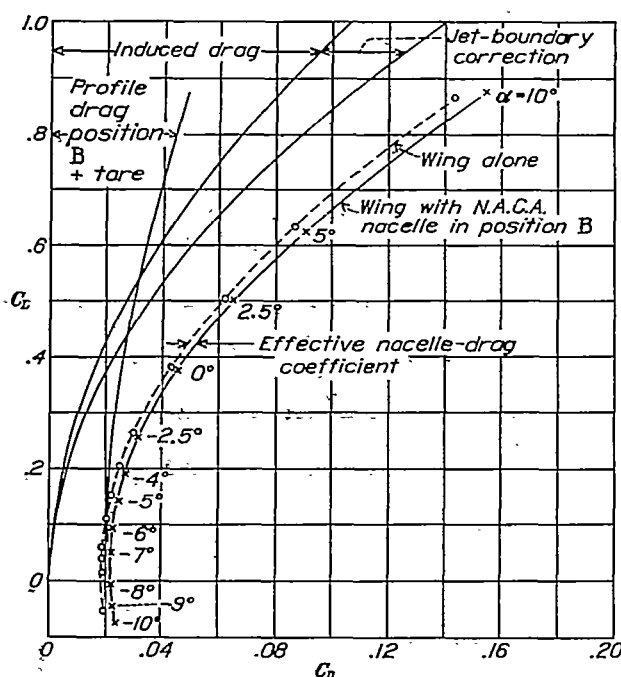


FIGURE 2.—Airfoil curves, propeller removed.

nondimensional coefficients and symbols employed are given and defined as follows:

$$\begin{aligned}
 C_L &= \frac{\text{lift}}{qS} \text{ (propeller removed)} \\
 C_D &= \frac{\text{drag}}{qS} \text{ (propeller removed)} \\
 C_{L_P} &= \frac{\text{lift}}{qS} \text{ (propeller operating)} \\
 C_T &= \frac{(T - \Delta D)}{\rho n^2 D^4} = \frac{(R + D)}{\rho n^2 D^4} \\
 C_{T_{\text{corr.}}} &= \frac{R + D_L}{\rho n^2 D^4} \\
 C_P &= \frac{P}{\rho n^3 D^5} \\
 \eta &= \frac{(T - \Delta D)V}{P} = \frac{(R + D)V}{P} = \left(\frac{C_T}{C_P} \right) \frac{V}{nD} \\
 \eta_{\text{corr.}} &= \frac{(R + D_L)V}{P} = \left(\frac{C_{T_{\text{corr.}}}}{C_P} \right) \frac{V}{nD}
 \end{aligned}$$

$$C_s = \sqrt[5]{\frac{\rho V^5}{P n^2}} = \frac{V}{\sqrt[5]{C_P}}$$

where

q , dynamic pressure ($\frac{1}{2} \rho V^2$).

ρ , mass density of the air.

V , velocity.

S , area of the wing.

T , thrust of propeller operating in front of a body (tension in crankshaft).

R , resultant forward force.

D , drag at given angle with propeller removed.

D_L , drag with propeller removed at the lift obtained with the propeller operating (same dynamic pressure).

ΔD , change in drag of body due to action of propeller.

n , revolutions per unit time.

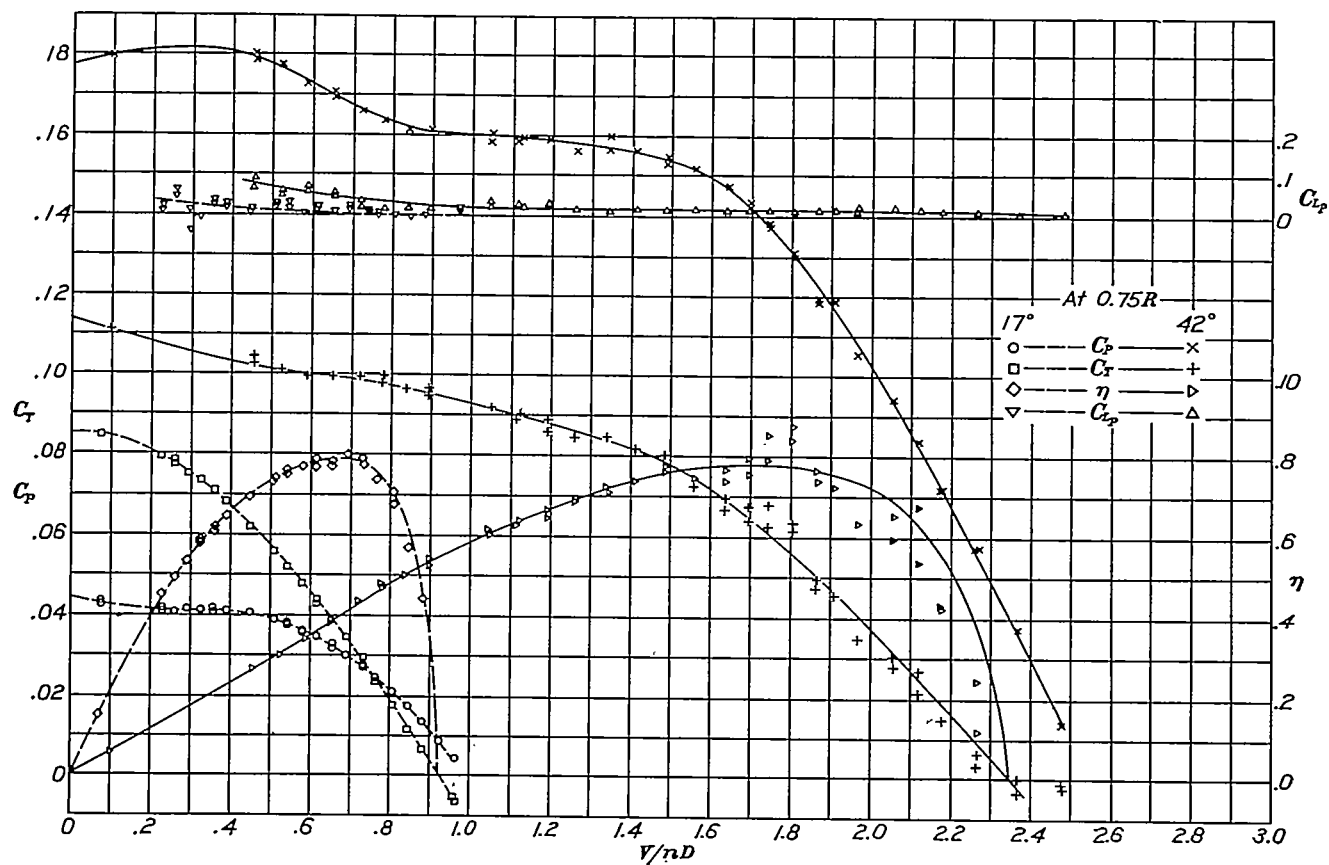
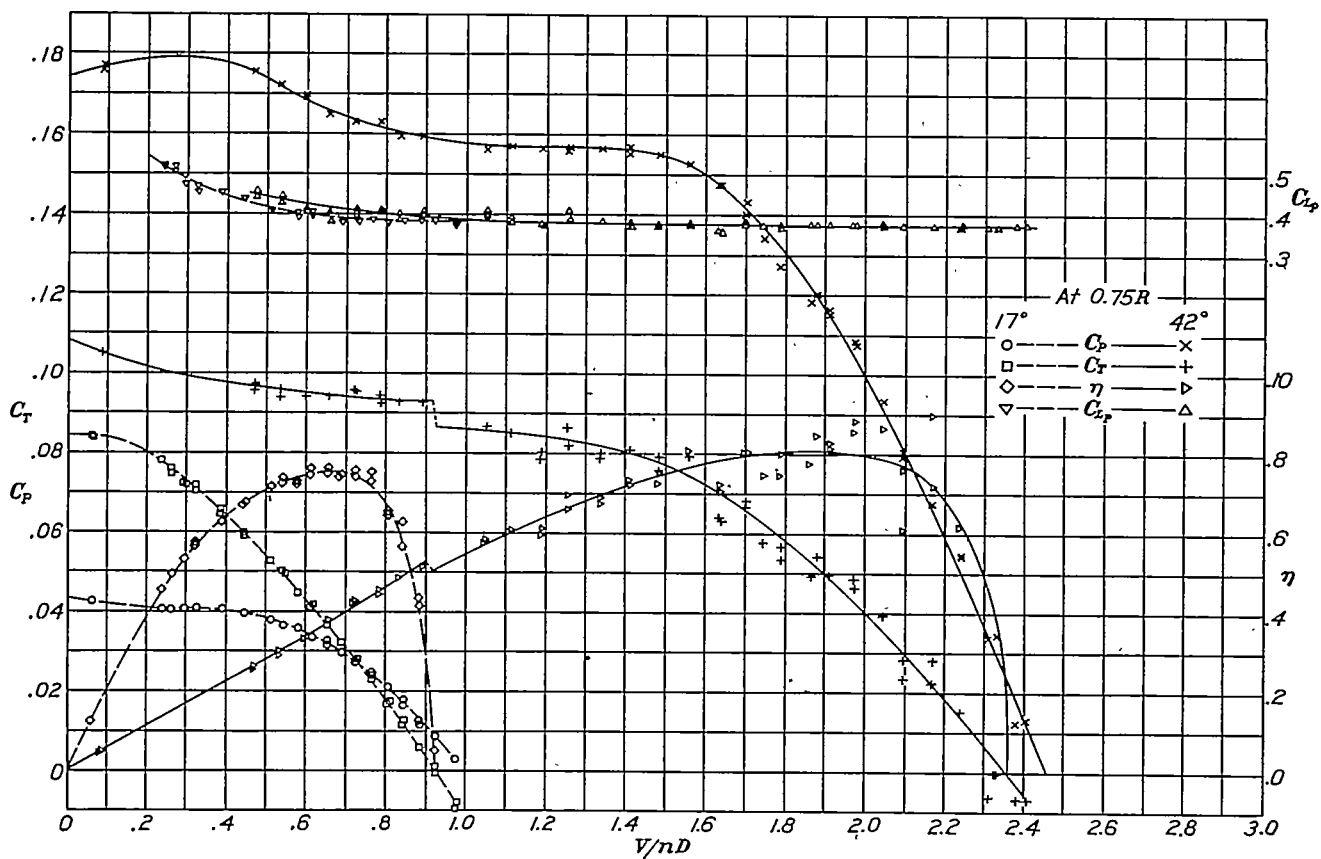
D , propeller diameter.

P , power.

The airfoil characteristics of the wing alone and for the wing with nacelle are given in figure 2. No tare corrections have been made. It should be noted that measurements have been made for close increments of angle of attack, especially in the region of minimum drag.

Although propeller tests were made at 17°, 22°, 27°, 32°, 37°, and 42° pitch at 0.75R at each of -8°, -5°, -2.5°, 0°, 2.5°, and 5° angle of attack, only a few sample test curves are shown. Figures 3 and 4, which are for the two extremes of pitch tested, show a considerable scattering of the test points, particularly of the thrust at the high pitch (42°). The power variations are largely a function of pitch, not angle of attack, and all power data are reliable, since the torque was measured directly and is not a computed value as is the thrust (thrust=resultant force + drag). The efficiency points, being computed from the thrust and power, show a dispersion similar to the thrust.

In tests of this type there is an inherent scattering of thrust-coefficient points at maximum efficiency and beyond, which increases as either the angle of attack or propeller pitch is increased. Three reasons exist for this dispersion. First, scattering occurs because the thrust, a computed value, is determined as the algebraic sum of the two measured quantities R and D . As zero thrust is approached these quantities are of the same order of magnitude but of opposite sign and consequently a small error in either may be a large percentage error in the effective thrust. Second, increasing the angle of attack, in addition to increasing the drag force, introduces correspondingly larger force fluctuations that are independent of propeller pitch. Third, and probably most important, in order to obtain the higher values of V/nD that correspond to higher pitches, the revolution speed of the propeller must be decreased because the tunnel air speed is

FIGURE 3.—Sample curves, uncorrected. Right-hand propeller No. 4412, 4-foot diameter, $\alpha = -8^\circ$.FIGURE 4.—Sample curves, uncorrected. Right-hand propeller No. 4412, 4-foot diameter, $\alpha = 0^\circ$.

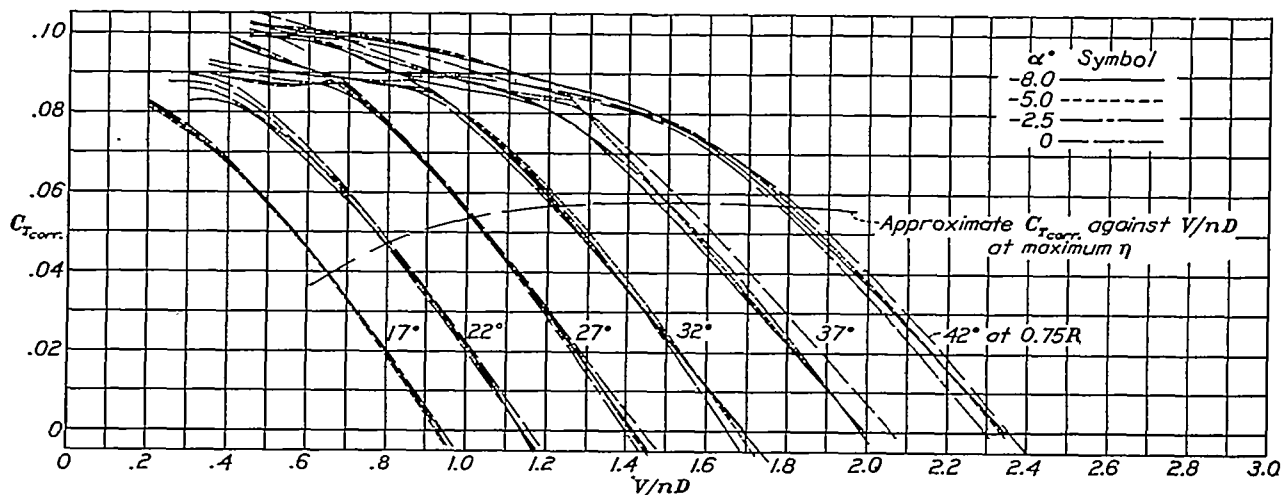


FIGURE 5.—Composite of corrected thrust. Right-hand propeller No. 4412, 4-foot diameter.

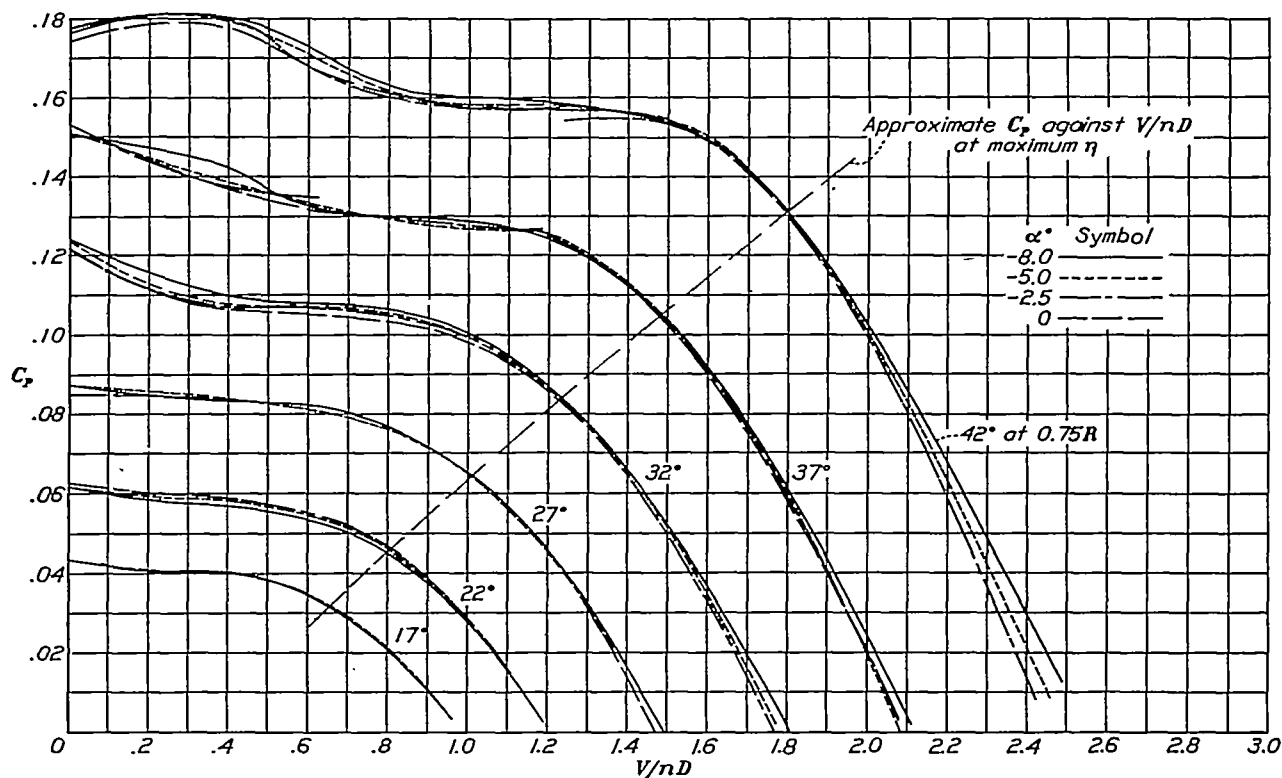


FIGURE 6.—Composite of power. Right-hand propeller No. 4412, 4-foot diameter.

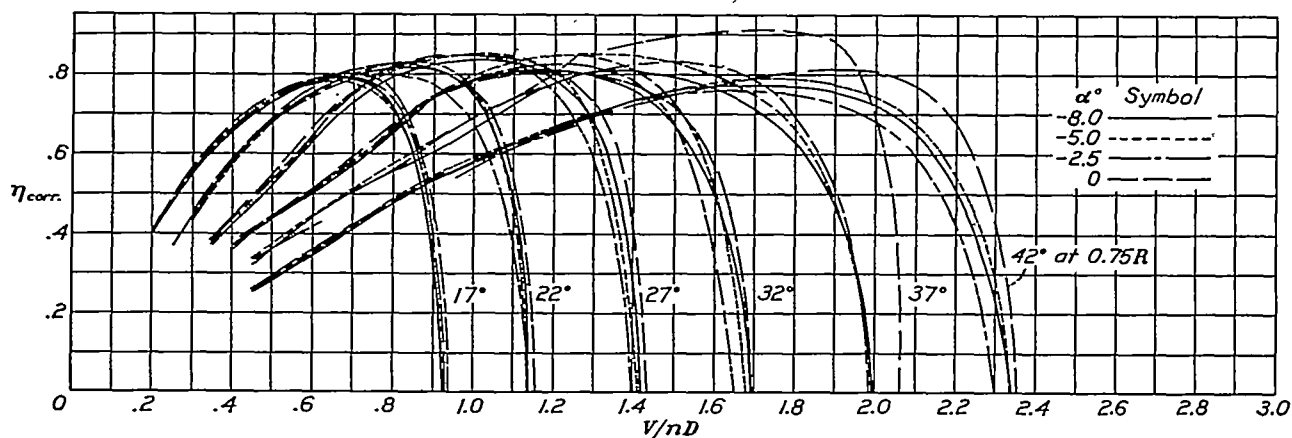


FIGURE 7.—Composite of corrected propulsive efficiency. Right-hand propeller No. 4412, 4-foot diameter.

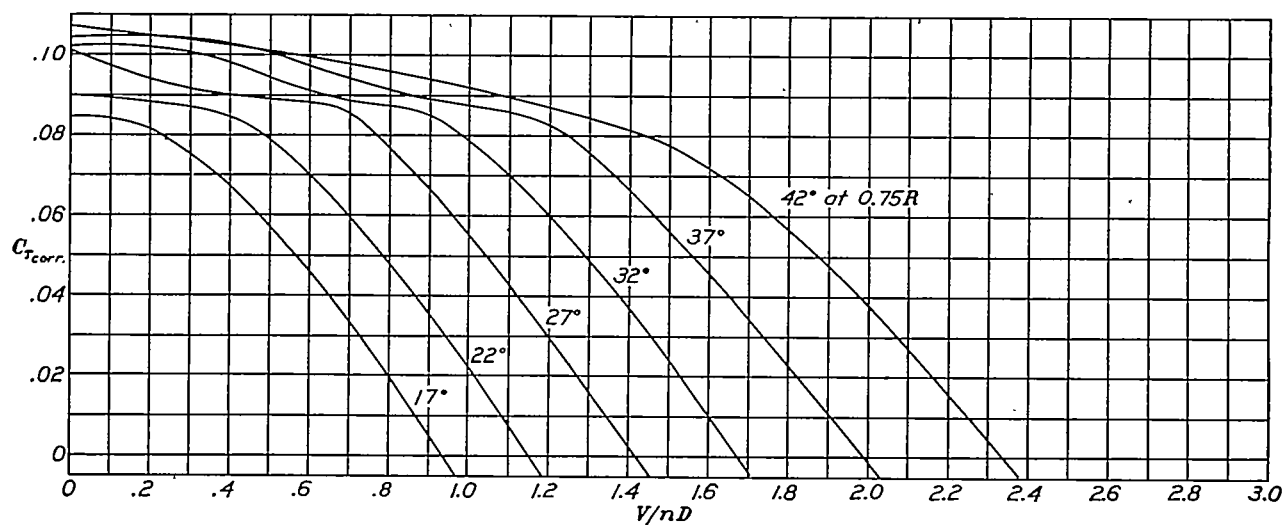


FIGURE 8.—Average corrected thrust. Right-hand propeller No. 4412, 4-foot diameter.

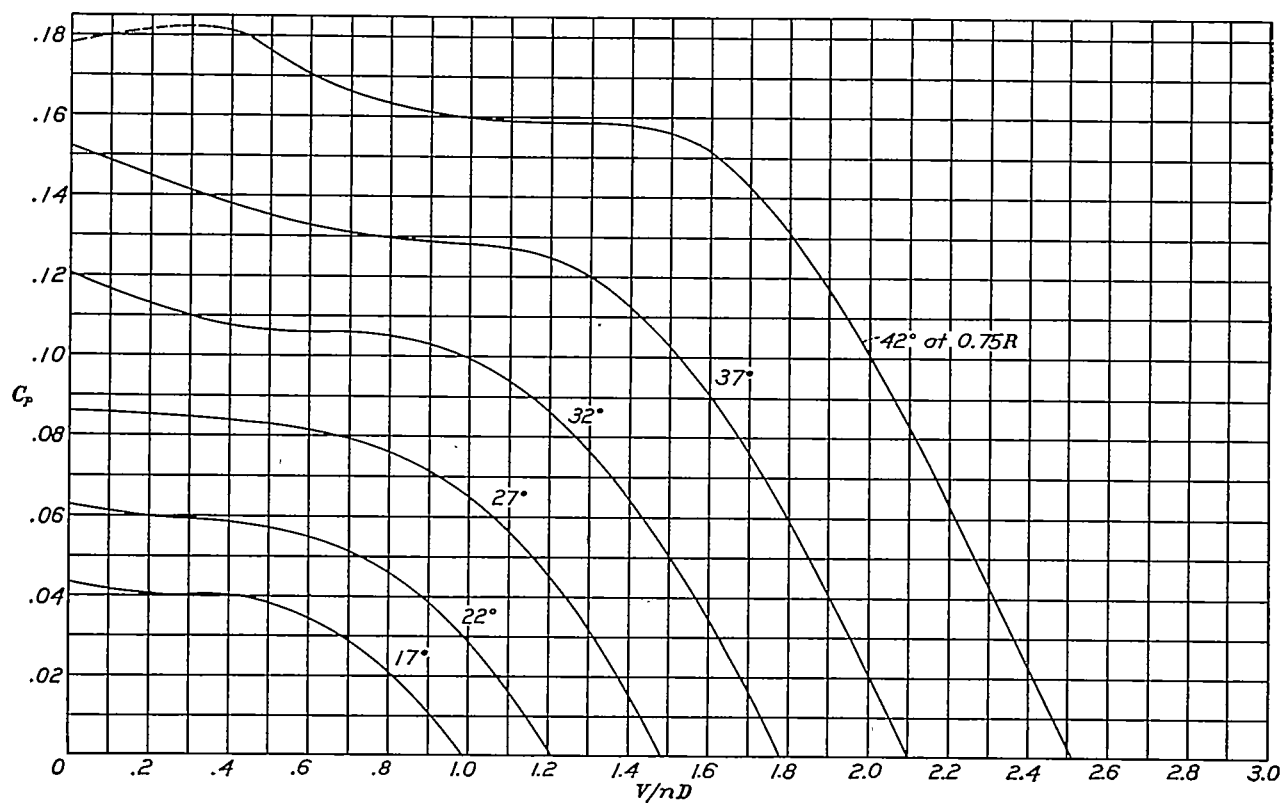


FIGURE 9.—Average power. Right-hand propeller No. 4412, 4-foot diameter.

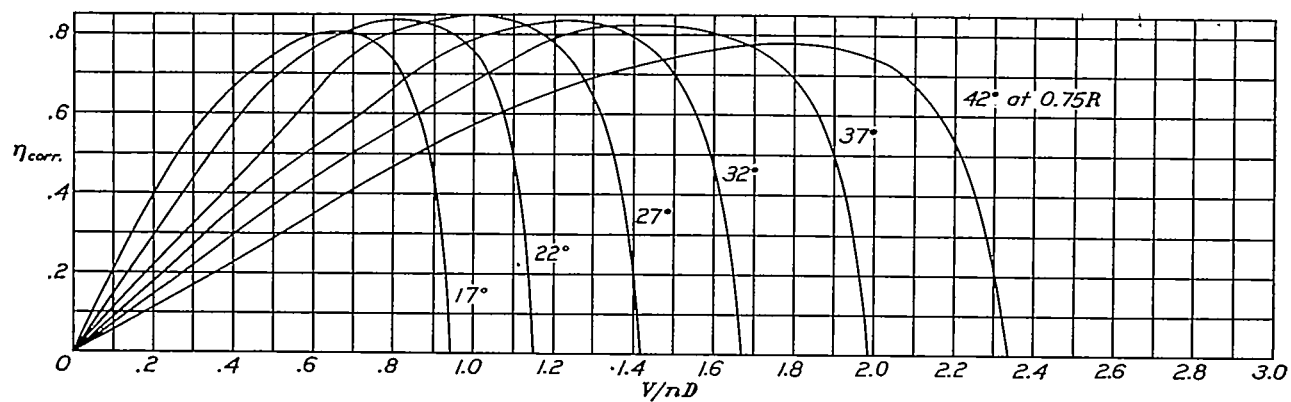


FIGURE 10.—Average corrected propulsive efficiency. Right-hand propeller No. 4412, 4-foot diameter.

limited. As the thrust coefficient varies directly as the thrust and inversely as n^2 , the scattering with propeller pitch will vary roughly as $(V/nD)^2$ for the same value of thrust coefficient and the same value of

pitch as at the lowest. The curves for the 37° propeller pitch at 0° angle of attack of the wing are an example of what would result if most of the test points were obtained under adverse conditions resulting from

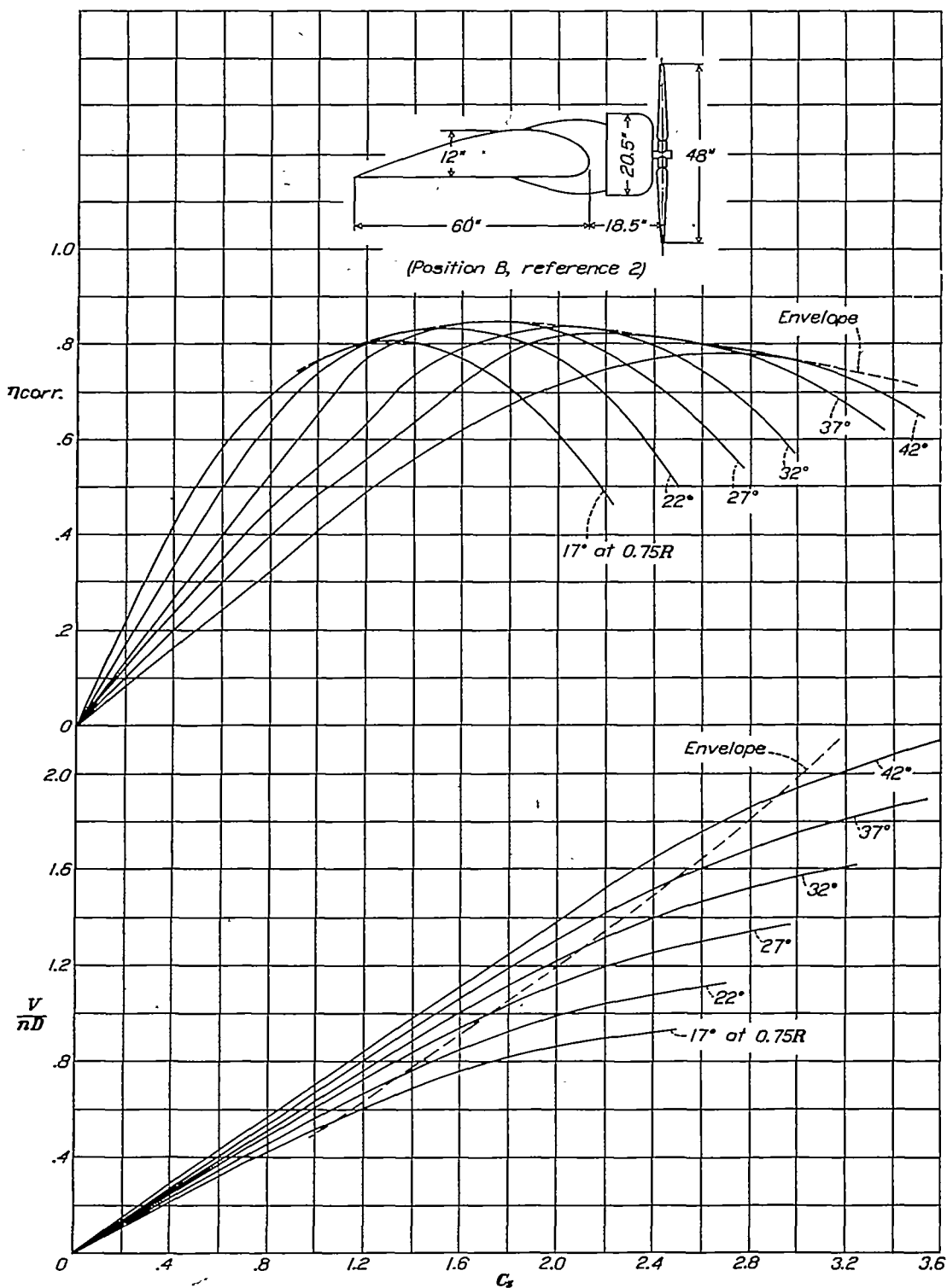


FIGURE 11.—Working chart, N. A. C. A. nacelle in line with thick wing. Right-hand propeller No. 4412, 4-foot diameter.

force fluctuations. On this basis the fluctuations of the thrust coefficient would increase with pitch and would be from 4 to 10 times as great at the highest

the three reasons discussed. The thrust is high and the effect on the efficiency is more obvious; this thrust curve was omitted in obtaining average values.

METHOD OF ANALYSIS

A full discussion of the difficulties and methods of comparing wing-nacelle-propeller combinations is given in references 2 and 4 and need not be repeated here. The "corrected propulsive efficiency" was introduced in reference 4 and is the basis on which these data are analyzed.

Figures 5, 6, and 7 are composite curves of corrected thrust, power, and corrected propulsive efficiency for all the pitches tested from -8° to 0° angle of attack of the wing; the curves for 2.5° and 5° are not included on account of the scattering of points previously mentioned. These data have been corrected similarly to those of reference 4 except that, instead of computing the difference in induced drag and jet-boundary correction, it was read directly from figure 2 and therefore includes a slight change in profile drag. This method of correction, considered admissible since previous tests have shown the tare drag to be independent of the lift, gives slightly higher values of thrust and efficiency than the method of reference 4, which assumes no change in profile drag. The difference in thrust and efficiency obtained by these two methods is small, especially near maximum efficiency, and certainly does not exceed the limits of accuracy of the tests.

The composite curves in figures 5, 6, and 7 indicate that, up to 0° angle of attack, the limit to which the data are considered to be reliable, the corrected thrust, power, and corrected propulsive efficiency are independent of angle of attack. Average curves were accordingly drawn from figures 5 and 6, omitting the thrust for 37° pitch at 0° angle of attack. Figures 8 and 9 show these average values of thrust and power and figure 10 shows the recomputed corrected propulsive efficiency, based on the foregoing averages. Table I lists these values together with the computed value of the operating coefficient C_s .

Figure 11 presents the data of table I in working-chart form. Figure 12 is a plot of C_{Lp} against C_s giving average values for all pitches. Table II lists values read from figure 12.

DISCUSSION

The airfoil curves for the wing alone and the wing with nacelle as shown in figure 2 are conventional. In general, the effective nacelle-drag coefficient at a constant lift is in good agreement with that of reference 2. Although the effective nacelle-drag coefficient varies somewhat with lift, it may be taken as 0.0026 for this combination over the high-speed range of flight.

Figure 7 indicates a tendency of the corrected propulsive efficiency to increase with angle of attack. This same trend is also shown by the data in reference 2 when the corrected propulsive efficiency is computed. Over the high-speed and climbing range of lift coefficients the change in corrected propulsive efficiency

is small, being almost within the accuracy of the experiments. The corrected propulsive efficiency may therefore be considered to be independent of the angle of attack except in very special cases and may be taken as the average over the high-speed and the climbing range.

The working chart given in figure 11 is to be used in the same manner as those of reference 1. This chart is, of course, based on certain fixed test conditions and in its application due allowances should be made for the effects of changes in propeller diameter, power input, and other variables.

The effect of the propeller on the lift is shown in figure 12. The curves apply only to these particular test conditions and must not be considered to have general application. They have been inserted to give the change in lift caused by the propeller and also to show that for a given arrangement the effect of propeller pitch is slight with a fixed-diameter propeller at constant values of C_s . No test points (see figs. 3 and

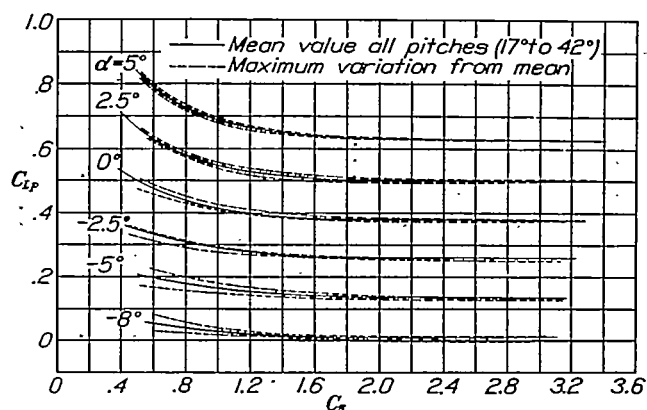


FIGURE 12.—Effect of propeller on lift.

4) are given, but the maximum variation of the faired curves for each pitch is shown. The small effect of propeller pitch may seem unusual but a few simple computations at the different pitches, assuming C_s , velocity, propeller diameter, and angle-of-attack constant, will show that the thrust is about the same for all pitches and, since the change in lift for any combination is mainly a function of propeller thrust, it is not unreasonable that the lift variation with propeller pitch should be small.

These are the first published results of tests made in the propeller-research tunnel of propellers at pitches greater than about 27° at $0.75R$. It is hoped that they may be useful in indicating trends for higher pitches from previous tests for lower pitches as well as be useful to the designer of modern high-speed airplanes. The reason for the falling off in efficiency as early as 27° is not fully explained. One possibility is that there may be increasing interference with the wing as the pitch of the propeller is increased. Available data (reference 5) covering the values of propeller pitches only up to 23° provide evidence that the tendency of

the wing interference is to increase as the propeller pitch is increased. The pitch distribution of the propeller used in this investigation is not considered particularly good for the higher pitches and a series of full-scale tests with more favorable pitch distribution is contemplated. It is expected that some improvement in the efficiency in the higher pitch range can be obtained.

LANGLEY MEMORIAL AERONAUTICAL LABORATORY,
NATIONAL ADVISORY COMMITTEE FOR AERONAUTICS,
LANGLEY FIELD, VA., November 12, 1935.

REFERENCES

1. Weick, Fred E.: Working Charts for the Selection of Aluminum Alloy Propellers of a Standard Form to Operate

with Various Aircraft Engines and Bodies. T. R. No. 350, N. A. C. A., 1930.

2. Wood, Donald H.: Tests of Nacelle-Propeller Combinations in Various Positions with Reference to Wings. Part I. Thick Wing—N. A. C. A. Cooled Nacelle—Tractor Propeller. T. R. No. 415, N. A. C. A., 1932.

3. Weick, Fred E., and Wood, Donald H.: The Twenty-Foot Propeller Research Tunnel of the National Advisory Committee for Aeronautics. T. R. No. 300, N. A. C. A., 1928.

4. Wood, Donald H., and Bioletti, Carlton: Tests of Nacelle-Propeller Combinations in Various Positions with Reference to Wings. VI—Wings and Nacelles with Pusher Propeller. T. R. No. 507, N. A. C. A., 1934.

5. Weick, Fred E., and Wood, Donald H.: The Effect of the Wings of Single Engine Airplanes on Propulsive Efficiency as Shown by Full Scale Wind Tunnel Tests. T. N. No. 322, N. A. C. A., 1929.

TABLE I.—AVERAGE VALUES

[Corrected for lift]

[Right-hand propeller No. 4412, 4-foot diameter]

V/nD	Set 17° at 0.75 R				Set 22° at 0.75 R				Set 27° at 0.75 R				Set 32° at 0.75 R				Set 37° at 0.75 R				Set 42° at 0.75 R			
	C _{T_{corr}}	C _P	η _{corr}	C _S	C _{T_{corr}}	C _P	η _{corr}	C _S	C _{T_{corr}}	C _P	η _{corr}	C _S	C _{T_{corr}}	C _P	η _{corr}	C _S	C _{T_{corr}}	C _P	η _{corr}	C _S	C _{T_{corr}}	C _P	η _{corr}	C _S
0	0.0846	0.0433	0	0	0.0900	0.0628	0	0	0.1010	0.0862	0	0	0.1020	0.1208	0	0	0.1043	0.1633	0	0	0.1070	0.1780	0	0
0.05	0.0848	0.0423	0.100	0.09	0.0893	0.0620	0.072	0.09	0.0990	0.0860	0.057	0.08	0.1022	0.1187	0.043	0.08	0.1046	0.1605	0.035	0.07	0.1067	0.1789	0.030	0.07
0.10	0.0842	0.0417	0.202	0.19	0.0890	0.0612	0.145	0.17	0.0970	0.0853	0.113	0.16	0.1023	0.1167	0.088	0.15	0.1047	0.1486	0.070	0.15	0.1060	0.1797	0.059	0.14
0.15	0.0831	0.0410	0.304	0.28	0.0887	0.0607	0.219	0.26	0.0954	0.0853	0.167	0.25	0.1021	0.1148	0.134	0.23	0.1048	0.1467	0.107	0.22	0.1054	0.1805	0.087	0.21
0.20	0.0817	0.0408	0.400	0.38	0.0881	0.0600	0.294	0.35	0.0940	0.0850	0.222	0.33	0.1019	0.1130	0.180	0.31	0.1047	0.1449	0.144	0.29	0.1049	0.1819	0.115	0.28
0.25	0.0786	0.0403	0.489	0.47	0.0877	0.0593	0.370	0.44	0.0927	0.0849	0.274	0.41	0.1012	0.1113	0.228	0.39	0.1043	0.1430	0.182	0.37	0.1042	0.1822	0.143	0.35
0.30	0.0750	0.0404	0.556	0.57	0.0870	0.0591	0.441	0.53	0.0918	0.0844	0.326	0.49	0.1005	0.1100	0.274	0.47	0.1040	0.1413	0.220	0.44	0.1035	0.1825	0.170	0.42
0.35	0.0711	0.0403	0.618	0.67	0.0860	0.0589	0.511	0.63	0.0909	0.0841	0.378	0.57	0.0993	0.1083	0.320	0.55	0.1033	0.1397	0.259	0.52	0.1030	0.1823	0.198	0.49
0.40	0.0670	0.0400	0.670	0.76	0.0844	0.0584	0.579	0.71	0.0900	0.0839	0.429	0.66	0.0980	0.1078	0.364	0.63	0.1028	0.1381	0.297	0.60	0.1022	0.1812	0.228	0.50
0.45	0.0621	0.0393	0.711	0.86	0.0821	0.0579	0.637	0.80	0.0894	0.0834	0.481	0.74	0.0961	0.1070	0.404	0.70	0.1018	0.1367	0.335	0.67	0.1017	0.1795	0.254	0.53
0.50	0.0571	0.0381	0.749	0.96	0.0788	0.0570	0.691	0.89	0.0890	0.0830	0.536	0.82	0.0942	0.1064	0.442	0.78	0.1006	0.1352	0.371	0.75	0.1009	0.1762	0.286	0.71
0.55	0.0518	0.0365	0.780	1.07	0.0745	0.0560	0.731	0.98	0.0837	0.0823	0.592	0.91	0.0926	0.1062	0.479	0.86	0.0990	0.1340	0.406	0.82	0.1000	0.1732	0.317	0.78
0.60	0.0459	0.0344	0.800	1.18	0.0699	0.0549	0.764	1.07	0.0800	0.0815	0.648	0.99	0.0910	0.1061	0.515	0.94	0.0971	0.1329	0.439	0.90	0.0992	0.1703	0.349	0.85
0.65	0.0395	0.0319	0.804	1.30	0.0649	0.0531	0.794	1.17	0.0773	0.0804	0.706	1.08	0.0898	0.1061	0.550	1.02	0.0967	0.1319	0.471	0.97	0.0983	0.1679	0.381	0.93
0.70	0.0330	0.0289	0.800	1.42	0.0594	0.0512	0.811	1.27	0.0742	0.0792	0.751	1.16	0.0888	0.1060	0.586	1.10	0.0940	0.1310	0.502	1.05	0.0975	0.1660	0.411	1.00
0.75	0.0261	0.0251	0.780	1.57	0.0540	0.0489	0.826	1.37	0.0718	0.0779	0.788	1.25	0.0880	0.1058	0.624	1.18	0.0928	0.1303	0.534	1.13	0.0968	0.1644	0.441	1.07
0.80	0.0192	0.0210	0.731	1.73	0.0479	0.0459	0.835	1.48	0.0700	0.0761	0.810	1.34	0.0873	0.1050	0.665	1.26	0.0913	0.1298	0.563	1.21	0.0959	0.1631	0.469	1.15
0.85	0.0121	0.0162	0.635	1.94	0.0416	0.0425	0.831	1.60	0.0720	0.0740	0.827	1.43	0.0866	0.1041	0.707	1.34	0.0902	0.1291	0.593	1.28	0.0950	0.1621	0.498	1.22
0.90	0.0049	0.0101	0.436	2.26	0.0351	0.0384	0.822	1.73	0.0682	0.0713	0.836	1.53	0.0850	0.1030	0.743	1.42	0.0890	0.1288	0.623	1.36	0.0939	0.1612	0.524	1.29
0.95	0.0028	0.0048	0.276	2.76	0.0285	0.0338	0.800	1.87	0.0608	0.0682	0.846	1.63	0.0821	0.1015	0.789	1.50	0.0881	0.1283	0.651	1.44	0.0929	0.1603	0.550	1.30
1.00					0.0218	0.0287	0.760	2.04	0.0549	0.0648	0.845	1.73	0.0783	0.0993	0.788	1.59	0.0874	0.1281	0.681	1.51	0.0919	0.1598	0.579	1.45
1.05					0.0148	0.0226	0.672	2.34	0.0488	0.0609	0.841	1.84	0.0742	0.0968	0.805	1.68	0.0868	0.1279	0.714	1.59	0.0908	0.1592	0.598	1.52
1.10					0.0072	0.0162	0.489	2.61	0.0426	0.0561	0.836	1.96	0.0698	0.0937	0.820	1.77	0.0858	0.1272	0.740	1.67	0.0896	0.1590	0.620	1.59
1.15					0.0001	0.0091	0.294	2.94	0.0360	0.0510	0.811	2.08	0.0650	0.0901	0.829	1.86	0.0844	0.1263	0.767	1.74	0.0883	0.1588	0.640	1.66
1.20					0.0292	0.0451	0.778	2.23	0.0292	0.0451	0.778	2.23	0.0600	0.0860	0.837	1.96	0.0825	0.1250	0.792	1.82	0.0871	0.1586	0.660	1.74
1.25					0.0226	0.0390	0.725	2.39	0.0226	0.0390	0.725	2.39	0.0545	0.0815	0.836	2.06	0.0797	0.1229	0.811	1.89	0.0858	0.1586	0.680	1.81
1.30					0.0158	0.0320	0.640	2.59	0.0158	0.0320	0.640	2.59	0.0488	0.0763	0.831	2.17	0.0765	0.1201	0.816	1.98	0.0841	0.1585	0.690	1.88
1.35					0.0091	0.0240	0.487	2.85	0.0091	0.0240	0.487	2.85	0.0428	0.0707	0.816	2.28	0.0716	0.1167	0.822	2.08	0.0829	0.1583	0.705	1.95
1.40					0.0023	0.0158	0.206	3.22	0.0023	0.0158	0.206	3.22	0.0368	0.0646	0.796	2.42	0.0681	0.1126	0.823	2.18	0.0813	0.1580	0.720	2.02
1.45					0.0000	0.0000	0.000	3.00	0.0000	0.0000	0.000	3.00	0.0304	0.0578	0.762	2.56	0.0612	0.1080	0.820	2.28	0.0795	0.1573	0.733	2.10
1.50					0.0239	0.0505	0.710	2.72	0.0239	0.0505	0.710	2.72	0.0239	0.0505	0.710	2.72	0.0562	0.1029	0.820	2.36	0.0777	0.1563	0.745	2.17
1.55					0.0170	0.0427	0.616	2.92	0.0170	0.0427	0.616	2.92	0.0170	0.0427	0.616	2.92	0.0510	0.0971	0.814	2.47	0.0750	0.1544	0.753	2.24
1.60					0.0102	0.0343	0.478	3.14	0.0102	0.0343	0.478	3.14	0.0102	0.0343	0.478	3.14	0.0456	0.0901	0.808	2.59	0.0720	0.1513	0.761	2.32
1.65					0.0031	0.0258	0.198	3.43	0.0031	0.0258	0.198	3.43	0.0031	0.0258	0.198	3.43	0.0400	0.0834	0.791	2.71	0.0687	0.1472	0.770	2.42
1.70					0.0000	0.0161	0.000	3.88	0.0000	0.0161	0.000	3.88	0.0000	0.0161	0.000	3.88	0.0342	0.0759	0.766	2.86	0.0651	0.1424	0.777	2.50
1.75					0.0285	0.0677	0.737	3.00	0.0285	0.0677	0.737	3.00	0.0285	0.0677	0.737	3.00	0.0285	0.0677	0.737	3.00	0.0611	0.1370	0.781	2.61
1.80					0.0228	0.0591	0.694	3.17	0.0228	0.0591	0.694	3.17	0.0228	0.0591	0.694	3.17	0.0228	0.0591	0.694	3.17	0.0568	0.1310	0.780	2.70
1.85					0.0188	0.0500	0.621	3.37	0.0188	0.0500	0.621	3.37	0.0188	0.0500	0.621	3.37	0.0188	0.0500	0.621	3.37	0.0521	0.1239	0.780	2.80
1.90					0.0108	0.0407	0.504	3.61	0.0108	0.0407	0.504	3.61	0.0108	0.0407	0.504	3.61	0.0108	0.0407	0.504	3.61	0.0474	0.1163	0.772	2.92
1.95					0.0047	0.0308	0.298	3.90	0.0047	0.0308	0.298	3.90	0.0047	0.0308	0.298	3.90	0.0047	0.0308	0.298	3.90	0.0424	0.1089	0.760	3.04
2.00					0.0012	0.0206	0.000	4.35	0.0012	0.0206	0.000	4.35	0.0012	0.0206	0.000	4.35	0.0012	0.0206	0.000	4.35	0.0373	0.1006	0.742	3.17
2.05					0.0321	0.0919	0.710	3.81	0.0321	0.0919	0.710	3.81	0.0321	0.0919	0.710	3.81	0.0321	0.0919	0.710	3.81	0.0289	0.0828	0.690	3.46
2.10					0.0268	0.0828	0.650	4.00	0.0268	0.0828	0.650	4.00	0.0268	0.0828	0.650	4.00	0.0268	0.0828	0.650	4.00	0.0211	0.0734	0.619	3.63
2.15					0.0158	0.0652	0.449	4.35	0.0158	0.0652	0.449	4.35	0.0158	0.0652	0.449	4.35	0.0158	0.0652	0.449	4.35	0.0158	0.0652	0.449	4.35
2.20					0.0069	0.0334	0.118	4.80	0.0069	0.0334	0.118	4.80	0.0069	0.0334	0.118	4.80	0.0069	0.0334	0.118	4.80	0.0069	0.0334	0.118	4.80
2.25					0.0011	0.0131	0.028	5.00	0.0011	0.0131	0.028	5.00	0.0011	0.0131	0.028	5.00	0.0011	0.0131	0.028	5.00	0.0011	0.0131	0.028	5.00
2.30					0.0000	0.0000	0.000	5.00	0.0000	0.0000	0.000	5.00	0.0000	0.0000	0.000	5.00	0.0000	0.0000	0.000	5.00	0.0000	0.0000	0.000	5.00
2.35					0.0000	0.0000	0.000	5.00	0.0000	0.0000	0.000	5.00	0.0000	0.0000	0.000	5.00	0.0000	0.0000	0.000	5.00				